Visualizing and quantifying biomineral preservation in fossil vertebrate dental remains (#87267)

First submission

Guidance from your Editor

Please submit by **18 Jul 2024** for the benefit of the authors (and your token reward) .

Structure and Criteria
Please read the 'Structure and Criteria' page for guidance.

Raw data check
Review the raw data.

Image check
Check that figures and images have not been inappropriately manipulated.

If this article is published your review will be made public. You can choose whether to sign your review. If uploading a PDF please remove any identifiable information (if you want to remain anonymous).

Files
Download and review all files from the materials page.

5 Figure file(s)
2 Table file(s)

Structure and Criteria

Structure your review

The review form is divided into 5 sections. Please consider these when composing your review:

1. **BASIC REPORTING**
2. **EXPERIMENTAL DESIGN**
3. **VALIDITY OF THE FINDINGS**
4. General comments
5. Confidential notes to the editor

You can also annotate this PDF and upload it as part of your review

When ready submit online.

Editorial Criteria

Use these criteria points to structure your review. The full detailed editorial criteria is on your guidance page.

BASIC REPORTING

- Clear, unambiguous, professional English language used throughout.
- Intro & background to show context. Literature well referenced & relevant.
- Structure conforms to PeerJ standards, discipline norm, or improved for clarity.
- Figures are relevant, high quality, well labelled & described.
- Raw data supplied (see PeerJ policy).

EXPERIMENTAL DESIGN

- Original primary research within Scope of the journal.
- Research question well defined, relevant & meaningful. It is stated how the research fills an identified knowledge gap.
- Rigorous investigation performed to a high technical & ethical standard.
- Methods described with sufficient detail & information to replicate.

VALIDITY OF THE FINDINGS

- **Impact and novelty is not assessed.** Meaningful replication encouraged where rationale & benefit to literature is clearly stated.
- All underlying data have been provided; they are robust, statistically sound, & controlled.
- Conclusions are well stated, linked to original research question & limited to supporting results.

Standout reviewing tips

The best reviewers use these techniques

Tip	*Example*
Support criticisms with evidence from the text or from other sources	*Smith et al (J of Methodology, 2005, V3, pp 123) have shown that the analysis you use in Lines 241-250 is not the most appropriate for this situation. Please explain why you used this method.*
Give specific suggestions on how to improve the manuscript	*Your introduction needs more detail. I suggest that you improve the description at lines 57- 86 to provide more justification for your study (specifically, you should expand upon the knowledge gap being filled).*
Comment on language and grammar issues	*The English language should be improved to ensure that an international audience can clearly understand your text. Some examples where the language could be improved include lines 23, 77, 121, 128 – the current phrasing makes comprehension difficult. I suggest you have a colleague who is proficient in English and familiar with the subject matter review your manuscript, or contact a professional editing service.*
Organize by importance of the issues, and number your points	*1. Your most important issue* *2. The next most important item* *3. …* *4. The least important points*
Please provide constructive criticism, and avoid personal opinions	*I thank you for providing the raw data, however your supplemental files need more descriptive metadata identifiers to be useful to future readers. Although your results are compelling, the data analysis should be improved in the following ways: AA, BB, CC*
Comment on strengths (as well as weaknesses) of the manuscript	*I commend the authors for their extensive data set, compiled over many years of detailed fieldwork. In addition, the manuscript is clearly written in professional, unambiguous language. If there is a weakness, it is in the statistical analysis (as I have noted above) which should be improved upon before Acceptance.*

Visualizing and quantifying biomineral preservation in fossil vertebrate dental remains

Matthew Cowen [Corresp., 1], **Marc de Rafélis** [2], **Loïc Ségalen** [3, 4], **Benjamin Kear** [5], **Maïtena Dumont** [6], **Zivile Zigaite** [Corresp. 1]

[1] Department of Organismal Biology, Uppsala University, Uppsala, Sweden

[2] UMR5563 Université de Toulouse/CNRS/IRD/Université Paul Sabatier,, Géosciences Environnement Toulouse (GET),, Toulouse, France

[3] Universite Rouen Normandie, Universite Caen Normandie, CNRS Normandie Universite, Rouen, Normandy, France

[4] UMR 7193, ISTEP, Sorbonne Université-CNRS, Paris, France

[5] Evolution Museum, Palaeontology and Minerology, Uppsala University, Uppsala, Sweden

[6] Laboratory of Bone Biomechanics, Koret School of Veterinary Medicine, The Hebrew University of Jerusalem, Jerusalem, Israel

Corresponding Authors: Matthew Cowen, Zivile Zigaite
Email address: Matthew.cowen@ebc.uu.se, Zivile.zigaite@ebc.uu.se

In this study, we attempt to illustrate fossil vertebrate dental tissue geochemistry and, by inference, the state of apatite preservation using quantitative, semi-quantitative and optical tools to evaluate bioapatite preservation. We present visual comparison of elemental compositions in fish and plesiosaur dental remains ranging in age from Silurian to Cretaceous, based on a combination of micro-scale optical cathodoluminescence (CL) observations (optical images and scanning electron microscope) with in-situ minor, trace and rare earth element (REE) compositions (EDS, maps and profiles, REE), as a tool for assessing diagenetic processes and biomineral preservation during fossilization of vertebrate dental apatite. Tissue-selective REE values have been obtained using Laser Ablation Inductively Coupled Plasma Mass Spectrometry (LA-ICP-MPS), indicating areas of potential REE enrichment, combined with Cathodoluminescence (CL) analysis. Energy Dispersive X-ray Spectroscopy (EDS) mapping was used to identify major elemental components and identify areas of contamination or diagenetic replacement. We conclude that the relative abilities of different dental tissues to resist alteration and proximity to the exposure surface reflect the REE composition and subsequently the inferred quality of preserved bioapatite.

Visualizing and quantifying biomineral preservation in fossil vertebrate dental remains

Matthew Bodle Cowen[1*], Marc de Rafélis[2], Loïc Ségalen[3,4], Benjamin P. Kear[5], Maïtena Dumont[6], and Živilė Žigaitė[1*]

[1] Subdepartment of Evolution and Development, Department of Organismal Biology, Uppsala University; Norbyvägen 18A, 75236 Uppsala, Sweden.
[2] Géosciences Environnement Toulouse (GET), UMR5563 Université de Toulouse/CNRS/IRD/Université Paul Sabatier, Observatoire Midi-Pyrénées, 31400 Toulouse, France.
[3] UMR 7193, ISTEP, Sorbonne Université-CNRS, Campus Jussieu, Tour 56-55, 5ème étage, 4 place Jussieu, 75252 Paris Cedex 05, France.
[4] UMR 6143, M2C, Université Rouen Normandie, Université Caen Normandie, CNRS Normandie Université, 76000 Rouen, France.
[5] The Museum of Evolution, Uppsala University; Norbyvägen 16, 75236 Uppsala, Sweden.
[6] Laboratory of Bone Biomechanics, Koret School of Veterinary Medicine, The Robert H. Smith Faculty of Agriculture, Food and Environment, HUJI, Rehovot, Israel.

*Corresponding Authors:

Matthew Bodle Cowen[1], Živilė Žigaitė[1;] Subdepartment of Evolution and Development, Department of Organismal Biology, Uppsala University; Norbyvägen 18A, 75236 Uppsala, Sweden.
Email addresses: Matthew.Cowen@ebc.uu.se; Zivile.Zigaite@ebc.uu.se.

Introduction

Assessing the preservation quality of fossil hard tissues such as bone, dentine, enamel or enameloid is fundamental to research that utilizes this material as a source of biogeochemical data. Isotopic and elemental proxies derived from fossil bioapatite rely on unaltered specimens to accurately reflect palaeobiology or the environmental conditions in the past. The chemical composition of fossil bone tissues, including trace elements and stable light isotope ratios, may provide valuable information on the biology of extinct species, such as thermometabolism (e.g. Amiot *et al.* 2007; Bernard *et al.* 2010; Eagle *et al.* 2011; Rey *et al.* 2017; Séon *et al.* 2020; Leuzinger *et al.* 2022), diet (e.g. Heuser *et al.* 2011; Owocki *et al.* 2020; Klock *et al.* 2022), ecology and environments (e.g. ~~Daniel~~ Bryant & Froelich 1995; Fricke *et al.* 2008; Amiot *et al.* 2010; Goedert *et al.* 2018, 2020; De Rooij *et al.* 2022; Thibon *et al.* 2022). Our ability to make such inferences depends on the preservation quality of the fossil remains, and at present there exists no definitive methodology for screening out digenetic alteration.

To better understand the effects of diagenesis and to discriminate the primary (or closest-to-primary) geochemical signal from secondary overprinting, a spatially resolved compositional analysis of the histological sections of fossil bioapatite is required. In this study we combine spectroscopic mapping techniques including cathodoluminescence (CL) and Energy dispersal spectroscopy (EDS) analysis with *in-situ* rare earth element (REE) analysis to visualize compositional changes. We examine plesiosaur teeth and lungfish dental plates from the Lower Cretaceous, as well as Devonian fish scales to compare potential biomineral preservation in enamel, enameloid, and dentinous tissues.

The mineral component of vertebrate hard tissues is composed of biological apatite, commonly present in the form of carbonate hydroxyapatites, which stabilize to fluorapatite

[$Ca_5(PO_4)_3F$] during diagenesis as the carbonate component diminishes and is replaced by fluorine (Trotter & Eggins, 2006; Keenan *et al.,* 2015; Lübke *et al.,* 2017). Depending on the conditions and environment of burial, the processes of fossilization may lead to the modification of preserved biominerals through ionic exchange and rearrangements in the primary structure throughout the incorporation of foreign ions in the crystal lattice. These ions may include rare earth elements (REE) for Ca^{2+} in Ca sites (Burton & Wright 1995; ~~Daniel~~ Bryant & Froelich 1995; Trueman & Tuross 2002; Trueman *et al.* 2006; Kocsis, Trueman & Palmer 2010; Heuser *et al.* 2011).

REE composition of fossil vertebrate hard tissues is an established tool for determining the extent of reworking and chemical changes during taphonomy (Trueman, 1999, 2013; Kohn & Cerling, 2002). Rare earth elements are also commonly used in the reconstruction of past environments (Grandjean *et al.* 1987; Kemp & Trueman 2003; Lécuyer, Reynard & Grandjean 2004; Fadel *et al.* 2015; Žigaitė *et al.* 2016; Ivanova *et al.* 2022), principally as a proxy to provenance, taphonomy and diagenesis. The incorporation of REEs and other trace elements into bioapatite predominantly takes place post-mortem (Toyoda & Tokonami, 1990) due to the infiltration from either sediment pore water, or directly from surrounding water bodies.

Apatite, with its very high affinity for REE, frequently contains at least two to three orders of magnitude higher REE concentrations than any other mineral phase present in the fossil bones and teeth (Trueman & Palmer 1997; Kohn, Schoeninger & Barker 1999; Trueman 1999). Concentrations of REE in fossil apatite from marine basins are higher than any other sedimentary mineral and commonly 5-6 orders of magnitude higher than seawater (Kolodny *et al.,* 1996). The REE reside in the two calcium sites in the apatite lattice and are normally present in living bone

at the ppb level (Shaw & Wasserburg 1985), while fossil bones yield much higher REE levels, usually in the 10^3 ppm range (Kolodny *et al.* 1996).

The REE record is taxon-independent since the REE do not appear to be physiologically vital trace elements and *in vivo* bone concentrations are several orders of magnitude lower than diagenetic concentrations (Trueman 1999). Wright *et al.* (1987) argued that ichthyoliths (disarticulated dermal and dental fish remains), concentrated at the sediment-water interface, exhibit an enrichment in REE, with no discernible fractionation of REE occurring during this particular process. However, ~~(Reynard *et al.* 1999)~~ convincingly argue for fractionation between seawater and ichthyoliths. Debate remains (summarized in Ivanova *et al.* 2022) as to whether REE uptake occurs only during early diagenesis or whether the process occurs continually. Two main mechanisms exist for REE trapping in phosphates – adsorption and substitution (Reynard *et al.* 1999; Trueman & Tuross 2002).

However, the adsorption process is in equilibrium and desorption of REE^{3+} ions can occur over time as argued by Li *et al.* (2021). Herwartz *et al.* (2011, 2013a, 2013b) have disputed the view set out by Reynard *et al.* (1999) that adsorption and substitution represent "early" and "late" stages of diagenesis. Further, Chen *et al.* (2015) have shown that in order to capture the composition of contemporary seawater, REE adsorption must occur close to the sediment-water interface, as even shallow burial can result in fractionation during early diagenesis.

Cathodoluminescence (CL) is achieved through the excitation of the sample mineral with a continuous high-energy electron beam to produce photon emission, generally in the visible spectra (Barbin 2013). CL analysis has been used extensively as a tool to assess preservation quality and diagenetic impact in fossil enamel (e.g. Götze *et al.* 2001; Schoeninger *et al.* 2003; Ségalen *et al.* 2008; Owocki *et al.* 2020; Richard *et al.* 2022). In assessing biomineral

preservation in apatitic fossil hard tissues, CL provides relatively quick tool to identify areas of diagenetic replacement (Ségalen *et al*. 2008), without further destruction of the thin section.

Substitution by other elements of Ca sites in the crystal lattice of apatite can be detected through CL, with the elements responsible for the substitution discernible based on the wavelength and hue of the photon emission. Substitution by Mn^{2+} produces a yellow or orange hue (Gaft *et al.* 1997) of between 565 nm and 585 nm. Unaltered biogenic apatite emits a dull blue luminescence of approximately 400nm (Schoeninger *et al.* 2003). Hättig *et al.* (2019) have shown that Mn^{2+} incorporation can cause CL emission in enamel from recent sharks, and thus CL alone cannot be relied upon as a diagenetic indicator. Areas of REE substitution were associated with distinct bands with sharp emission lines between 300nm and 1000nm (Gaft *et al.* 1997; Blanc *et al.* 2000; Habermann *et al.* 2000; Ségalen *et al*. 2008). Notably, Gaft *et al.* (1997) showed that the luminescence bands are absent where adsorption has occurred and are only present as a result of substitution.

EDS is a widely used SEM technique for determining the elemental composition of specimens. EDS has previously been used to study the distribution of elements within dental remains in relation their structure and functional use (e.g. Enax *et al.* 2012; Dumont *et al.,* 2009; Dumont *et al.* 2011) and to compare the element composition present in the teeth of different groups of organisms (Lübke *et al.* 2015).

LA-ICP-MS is *in-situ* mass spectroscopy with down-hole compositional depth profiling, which provides reliable quantitative high-resolution REE and major element compositions with only minor destruction of the thin section (see Trotter and Eggins 2006; Žigaitė *et al.* 2016).

In this study we use cathodoluminescence-microscopy and spectroscopy (micro-CL) combined with energy dispersive spectroscopy (EDS) and *in-situ* laser ablation inductive

coupled plasma mass-spectrometry (LA-ICP-MS) on fossil bioapatite, using ~~the~~ several types of dental fossils, and the same thin and thick sections to be able to combine and cross-verify the three techniques.

Materials & Methods

Samples investigated ~~by~~ this study include dermal scales from jawless and jawed fishes from the Devonian of Svalbard as well as plesiosaur tooth crowns and fossil lungfish (dipnoi) dental plates from the Cretaceous of SE Australia.

Figure 1

The Devonian fish scales were obtained from the palaeontological collections of Paris National Natural History Museum (Museum national d'Histoire naturelle), France. Original sampling of this material was from the Andrée Land Group of Spitsbergen Island, Svalbard archipelago, Norway. Scales analysed comprise two taxa, the thelodont *Talivalia svalbardae* and an undescribed putative chondrichthyan, both of which come from the Grey Hoek Formation in the upper part of the Andrée Land Group succession. The thelodont have been described by Žigaitė *et al.* in 2013, and the putative chondrichthyan by Žigaitė *et al*. ~~recently~~ (in prep).

The Early Cretaceous plesiosaur and lungfish fossils were sampled from the palaeontological collection of the Melbourne Museum (Museums Victoria) (NMV), Melbourne, Australia. One plesiosaur tooth and one lungfish toothplate (see Fig. 1) were selected from the lower Albian, the Eumeralla Formation and uppermost Barremian to lowermost Aptian, the Wonthaggi Formation of southeastern Australia (Wagstaff *et al.,* 2020). Previous taxonomic

143 evaluations of these plesiosaur teeth suggested leptocledian affinity (Kear, 2006; Kear &
144 Hamilton-Bruce, 2011; Poropat *et al.,* 2018, 2023; Kear *et al.,* 2018); the lungfish toothplates
145 cannot be confidently identified beyond Ceratodontiformes ~~indet~~ (see Poropat *et al.* 2018 for
146 discussion).
147 All specimen sections are held in The Museum of Evolution Palaeontological Collections
148 (PMU), Uppsala University, Sweden.
149
150 ***Geological settings***
151
152 *Svalbard material*
153 The thelodont and chondrichthyan scales used in this study come from the Andrée Land,
154 territory in the northern part of Spitsbergen Island, Svalbard archipelago. Stratigraphically the
155 material originates from the Lower Devonian Old Red Sandstone succession referred to as the
156 Andrée Land Group (Blomeier *et al.,* 2003) and represents deposition in a continental rift basin
157 along the northern margin of the Old Red Sandstone (ORS) landmass. The succession is
158 essentially confined to a major graben with a unique depositional history, involving a shift from
159 coarse clastic red-beds, mainly of alluvial fan and fluvial origin, to a series of more greyish
160 fluvial and possibly deltaic sediments illustrating the transition from the southern arid zone to the
161 equatorial tropics. The nature of the basin and the palaeoenvironmental conditions are as yet
162 poorly understood, although it plays an important role as a regional niche and separate
163 biogeographical province in the Early Devonian.
164 Vertebrate microfossils are quite common in the Andrée Land deposits, and include
165 isolated micromeric elements of the dermal exoskeleton (dentine scales) of acanthodians,

chondrichthyans, and thelodonts (Ørvig 1967; Blom & Goujet 2002; Žigaitė *et al.* 2013). The Formation extends from Lower to Middle Devonian (Blomeier *et al.* 2003). It is subdivided into three lithographical units: the Verdalen, Skamdalen and Tavlefjellet members (Blomeier *et al.* 2003; Volohonsky *et al.* 2008). The ~~Thelodont~~ scales come both from the Tavlefjellet and Skamdalen, while the undescribed chondrichthyan comes only from Skamdalen, Gråkammen locality (Žigaitė *et al.* 2013).

Australian material

The Wonthaggi and Eumeralla formations consist of fluvial sandstone and mudstone deposits which formed part of a wider floodplain arising from the rifting of mainland Australia, Tasmania and Antarctica (Mutter *et al.* 1985). Both formations have previously yielded a diverse array of vertebrate body and ichnofossils (Martin *et al.* 2012; Poropat *et al.* 2018; Romilio & Godfrey, 2022).

The informally designated ´Wonthaggi Formation` is a unit of Strzelecki Group correlated as latest Barremian to earliest Aptian on the basis of palynology (Wagstaff *et al.* 2020). The Eumeralla Formation from the Otway Group is early Albian in age (Wagstaff *et al.* 2020). The Wonthaggi Formation`records evidence of possible freezing in the winter (Wagstaff and Mason 1989) in contrast with more temperate conditions present in the Eumeralla Formation. Both units are associated with high palaeolatitudes, the position of Australia during the Lower Cretaceous being approximately 60-80^{o}S (Embleton & McElhinny 1982). An assessment of the floral communities of the Eumeralla Formation by Tosolini *et al.* (2018) concluded that a warmer climate may have ~~been~~ involved strong seasonal ~~variation~~.

189

190 *Sample Preparation*

191

192 Sectioning and preparation of dental fossils used in this study was carried out at the
193 Department of Organismal Biology at Uppsala University, Sweden and at the NordSIM facility,
194 Department of Mineralogy, Swedish Museum of Natural History, Stockholm, Sweden. Sections
195 were taken along the vertical axial plane of each tooth fragment, through both the enamel and the
196 dentine. The sample sections were selected on the basis of enamel thickness to provide a
197 reasonable amount of working material. Thin sections (30 μm) were polished and carbon-coated
198 before CL-spectroscopy analysis at the Biomineralizations and Palaeoenvironment group, the
199 ~~University of Pierre and Marie Curie~~ Paris 6, France. The same sections of plesiosaur teeth and
200 the dental plates of lungfish were subsequently analysed through SEM analysis.

201

202 *Energy Dispersive X-ray Spectroscopy (EDS)*

203

204 The chemical composition of the biomineral was investigated using Energy-Dispersive
205 X-Ray Spectroscopy (EDS) at the Max Plank Institute for Iron Research, Duesseldorf, Germany
206 in accordance with the method outlined in Dumont *et al.* (2014). EDS elemental map sections
207 and profiles have been generated for the plesiosaur teeth and the tooth plates of lungfish. SEM
208 imaging was conducted using a Jeol JSM-6500F scanning electron microscope operating at 15
209 kV with a tungsten filament instrument. The microscope was equipped with an EDAX-TSL
210 EBSD system. The chemical compositions used in mapping were determined using EDAX
211 energy-dispersive X-ray spectrometers (EDS) attached to the electron microscope. The

212 microanalyses were conducted using the EDAX library standard-less procedure with a 20 second
213 dwell time.
214
215 *Laser Ablation Inductively Coupled Mass Spectrometry (LA-ICP-MS)*
216
217 All specimens subject to LA-ICP-MS underwent gold ~~spattering~~ and polishing prior to
218 analysis. The elemental compositions were obtained by laser ablation inductively coupled plasma
219 mass spectrometry (LA-ICP-MS) at the Imaging and Analysis Centre of Science Facilities
220 Department, Natural History Museum, London (UK). LA-ICP-MS is a widely used technique to
221 determine in-situ mineral elemental compositions, and offers the necessary high spatial
222 resolution required to analyse REE and trace element compositions of micron-sized scales *in-situ*
223 at a separate tissue level. Analyses were performed using a New Wave Research UP213AI 213
224 nm aperture imaged laser ablation accessory coupled to a Thermo Elemental PQ3 ICP-MS with
225 an enhanced sensitivity S-option interface. Data were acquired for 120 seconds at each analysis
226 site on the plesiosaur and lungfish specimens, taking individual points in histologically different
227 regions (dentine or enamel). Background signals were collected for the first ca 60 s and the laser
228 fired at the sample to collect sample signals for the remaining acquisition time. Data were
229 collected using the time resolved method and were processed offline using LAMTRACE
230 software (Simon Jackson, Macquarie University, Sydney).
231 Elemental concentrations were calculated using the National Institute of Standards and
232 Technology (NIST) standard reference material 612 for calibration and calcium was used for
233 internal standardization. The limit of detection was taken as 1σ of the mean background count,
234 and the data filtered at twice this limit (2σ). Calculated precision was better than 3% RSD (at 1σ

error) when using ^{43}Ca as an internal standard. The concentrations of REEs were measured in parts per million and normalized to Post-Archaean Australian Shale (PAAS) concentration values (McLennan 1989). The obtained *in-situ* REE compositions are explored below using basic geochemical calculations and quantifications for sedimentary rocks (Reynard, Lécuyer and Grandjean 1999; Johannesson *et al.* 2006; Žigaitė *et al.* 2016 and citations therein). Elemental compositions were measured in parts per million (ppm), and the Al_2O_3, SiO_2, TiO_2, MgO, CaO, MnO and FeO oxides, in weight percentages (wt%) (see Supplementary Tables 1-7).

Optical cathodoluminescence

Optical CL examination of the samples was performed at the Imaging and Analysis Center (NHMUK) using an OPEA Catodym luminoscope at 15kV and 300-μA. Transmitted light and CL images of the samples were taken using a Nikon D70 digital camera. CL images were subsequently processed in Adobe Photoshop by raising brightness 150%. This was done to enhance the visibility of histological features as well as cracks, in order to visualize any changes in the distribution of secondary elements associated with these features. The luminescence colours and their corresponding wavelengths were then compared to the peak shifts for REE emission spectra (Ségalen *et al.,* 2008).

Results

Optical Cathodoluminescence

258 **Figure 2**

259

260 The optical CL images of the specimens from Eumeralla show a red-orange luminescence
261 present in the biomineralized tissue ~~all of~~ our samples, most likely attributable to REE
262 substitution in the Ca^{+} sites of the preserved apatite. Luminescence of this hue is associated with
263 replacement by Eu^{3+} and Sm^{2+} ions (Blanc *et al.* 2000, Ségalen *et al.* 2008). In the lungfish plate,
264 distinct areas of light blue or violet luminescence can be seen in the matrix infill around the
265 denteons (Fig. 2C). Light blue/violet luminescence is not exclusive to bioapatite, and occurs
266 number of silicate minerals (Götze, 2012). The EDS maps of this specimen (see supplementary
267 data) show enrichment of silicon and aluminium within this infill. These elements are not
268 signature of an original bioapatite, suggesting this luminescence is representative of secondary
269 mineral infilling rather than the preserved dentine.
270 In the Devonian fish from Svalbard, a yellow-orange luminescence is observed.
271 Substitution by Dy^{3+}, Sm^{3+}, and Eu^{3+} ions is associated with these hues (Blanc *et al.* 2000,
272 Ségalen *et al.* 2008). Notably, the interior pulp cavity in the thelodont scale from Tavlefjellet
273 (Fig. 2G) appears to luminesce a bright yellow, although filtered through the external enameloid.
274 Yellow luminescence can also arise from Mn^{2+} substitution, which may also contribute to this
275 effect. However, the overall concentration of MnO is lower in the Gråkammen scales in
276 comparison to the Tavlefjellet scale, as measured by *in-situ* LA-ICP-MS.
277 As optical cathodoluminescence imaging is limited to the visible spectrum of light,
278 luminescence in wavelengths outside the visible range is not detected. Thus, despite the
279 abundance of Gd in the specimens being comparable or exceeding that of Sm and Eu (Fig. 3, D)

the influence of this element on the CL images is not observed as the emission peak of the Gd^{3+} ion in apatite has a wavelength in the ultraviolet range (Blanc *et al.* 2000).

Trace element analysis

The EDS maps (Supplementary Figures) show that secondary elements are concentrated in areas accessible by pore fluids; most significantly in the dentine and internal pores and voids but also at the enamel-matrix interface and in cracks. Differences in secondary mineralization between the two formations appear to be minor and are best explained by the histology of the samples.

The plesiosaur teeth from Eumeralla exhibit a limited secondary element presence, with high calcium and phosphorous concentrations in both the dentine and enamel. Samples 1122A and 1122B both feature homogenous distribution of Ca and P across the enamel layers (Suppl. Figures). Secondary minerals are largely concentrated in and around cracks. No surficial inclusions are present in these samples.

The Eumeralla lungfish dental plates overall show more widespread secondary mineralization than the plesiosaur teeth, but with strong histological differentiation in the distribution of these minerals. For example, the enamel does not appear to have undergone significant secondary mineralization, both according to the REE concentrations, and the micro-CL and EDS imaging. Sample 1122C exhibits a slight reduction in calcium and phosphorous in areas of cracked enamel and in the vicinity of the enamel-dentine junction. Both 1122C and 1122D exhibit surficial inclusions of Si-, Al-, and ~~Na- based~~ minerals. By comparison, dentine contains a greater number of minerals present in relatively high concentration. The dentine of sample 1122D has been infiltrated by iron-, aluminium-, and ~~silicon- based~~ minerals which have

crystalized within cavities in the dentine. Outside of these cavities calcium and phosphorous remain abundant, with similar concentrations observed in both enamel and dentine.

REE Analysis

REE concentrations are highest in the dentine and lowest in the inner enamel of the plesiosaur teeth. The EDJ (enamel-dentine junction) generally has an REE content lower than the dentine but higher than the lower enamel. More REEs are present in the outer part of the enamel than in the inner part. This suggests that the samples experienced approximately the same degree of post-mortem crystallization, independent of age and burial environments. Contrastingly, in the Svalbard fish scales REE concentrations are substantially higher in the pulp cavity than the outer enameloid layers, with europium (Eu) anomalies present in all samples and tissue types.

Figure 3

Cerium (Ce) and Lanthanum (La) anomalies can be calculated based on the LA-ICP-MS data and represent an important paleoenvironmental indicator, as these anomalies are linked to the oxic state of pore waters (e.g. Reynard *et al.* 1999; Kemp & Trueman 2003; Patrick *et al.* 2004). Negative Ce anomalies are associated with oxic conditions, whilst positive anomalies - or the absence of an anomaly - may indicate anoxia. The shale-normalized cerium $(Ce/Ce^*)_{sn}$ and praseodymium $(Pr/Pr^*)_{sn}$ was calculated using the formula $Ce/Ce^* = 2Ce_{sn}/(Lasn + Nd_{sn})$ and $Pr/Pr^* = 2Pr_{sn}/(Ce_{sn} + Sm_{sn})$ (Barrat *et al.* 2023) (figure 4).

Figure 4

Discussion

Most of the enamel present in the samples studied appears to represent the original biomineralized material. The outermost enamel at the surface of the teeth and dental plates has a higher secondary element content than the inner enamel. The exposure of the outer surface of the hard tissues to the environment may account for this to some extent; it is the area with the most contact with the matrix fluids that are the source of many of the secondary elements. The presence of elevated REE concentrations on the outer enamel relative to the inner enamel is consistent with the observations of Williams *et al.* (1997) and Ségalen *et al.* (2008) that REE integration occurs primarily at the interface between the preserved tissue and the sediment. The density and poor permeability of the outer enamel may shield the inner matrix from pore fluid infiltration.

In the Wonthaggi plesiosaur teeth, secondary minerals are more prevalent. In sample 1223A the pulp cavity has undergone extensive infilling, with Al, Si, Fe and Zn present in higher concentrations than the surrounding dentine. The enamel of this sample is less secondarily mineralized, though infilling of cracks by Si and ~~Al- based~~ minerals is observed. Sample 1223B also exhibits some secondary mineralization. Whilst there is no infilling of the pulp cavity, the dentine is marked in places by areas of increased F and C; while Al, Si, and C fillings in the cracks of the inner part of the tooth surficial inclusions are observed, along with infiltrations of Fe at the outermost extent of the dentine. The lungfish plates display high levels of Ca and P, more so than is seen in the dentine of other samples. Secondary mineralization is present, with extensive infilling of pore spaces and dentine tubules by Si, Al, and Fe. Although infilling is

widespread, particularly in sample 1123D (Suppl. Figure 11), no large areas of recrystallisation as seen in the Eumeralla specimens.

In both sets of samples Si, Al and Fe are the most abundant elements present in cracks. The probable source of these elements is the matrix in which the specimens were deposited; the formations in which the specimens were found consist of sandstones and mudstones from which high quantities of quartz and clay minerals are to be expected. Fluorine (F) is generally elevated in fossil hard tissues relative to contemporary remains, as *in vivo* incorporation of F into bioapatites is comparatively low, while fluoride ions readily replace OH- during diagenesis (Ghadimi *et al.* 2013; Keenan *et al.* 2015). An exception would be enameloid, which has close chemical composition to geological fluorapatite (Sasagawa *et al.* 2009; Enax e*t al.* 2012). In our samples, F is present in the matrix and accumulates in areas close to surficial cracks, but is also present within the fossil tissue. The distribution of F within all the analysed tissues is largely homogenous, with no clear distinction between dentine and enamel visible from the EDS maps (see Supplementary data).

Secondary elements are marginally more prevalent in the lungfish plates than in the plesiosaur teeth. Lungfish do not shed their dental plates (Kemp 2002), and they are thus only deposited with the death of the animal. The outer surface of the plate is susceptible to mechanical wear which may expose the eroded dentine to secondary elements. Wearing may be exacerbated by environmental stresses such as food availability and Oxygen concentration (Kemp 2005). It should also be noted that some lungfish taxa replace eroded enamel with hydroxyapatite enriched petrodentine which is continuously produced (Smith & Krupina 2001; Kemp 2001). By contrast, plesiosaurs are known to have undergone continuous tooth shedding and replacement (Kear *et al.* 2017). Polyphyodonty (tooth shedding) is a trait found in the majority of vertebrate groups and is

not indicative of an animal's metabolism. Kear (2006) noted that the plesiosaur teeth used in this study also exhibited wear to some degree, though not to the extent that inclusions in worn enamel present a significant route for secondary mineral infiltration into the dentine compared to cracks or natural holes.

As with the secondary elements, luminescence is strongly associated with cracks and the outer surfaces of the samples, reflecting the vulnerability of these areas to infiltration by pore waters during diagenesis. The enamel present in the plesiosaur teeth superficially appears to luminesce more strongly than the dentine, contrary to expectation based on LA-ICP-MS results. We suggest this may result from the transparency of the enamel allowing for more photon transmission than in relatively opaque dentine rather than a signal of potential diagenetic infiltrations. The wavelength of the luminescence, inferred from the hue, is of greater importance to this study than the intensity as it is indicative of whether REE replacement has occurred. It is also suggestive of which elements may be responsible for said replacement, though this information is substantially less quantitative in comparison to methods such as LA-ICP-MS.

The compositional profiles obtained in the context of fossil tissue histology determines potential systematic trends in their relative permeability and susceptibility to diagenesis. Enamel and enameloid are more resistant to replacement and alteration than dentine as they are of a lower porosity and more extensively mineralised, with <2% organic content (Hoppe *et al.* 2003) in comparison to approximately 70% in dentine. Dentine is less mineralised than enamel and ~~conmposed~~ of micro-sized tubules which increase its porosity and permeability. In lungfish dental plates the dentine is also vascularized (Kemp & Barry, 2006), with voids left by blood vessels providing an entry-point for groundwater during taphonomy and early diagenesis. These

factors increase the potential for infiltration of the dentine by secondary elements, in turn increasing the likelihood of mineral alteration and replacement.

The strong yellow luminescence in the pulp cavity of the Tavlefjellet thelodont scale (Fig. 2G) suggests stronger infiltration of the cavity by REEs relative to the dentine and enameloid. This is supported by LA-ICP-MS analysis showing REE concentrations in the pulp, in particular Eu, up to an order of magnitude higher than in other tissues. Pulp is extensively vascularised and has a greater organic component than dentine, and so more susceptible to fluid infiltration. Greater REE enrichment of the pulp in comparison to the other tissues further supports the porosity of hard tissues being a significant factor in diagenetic REE uptake.

REE profiles are indicative of limited diagenetic alteration. In the plesiosaur teeth, the degree of preservation in the inner enamel is such that the isotope signal produced can be interpreted as primary. REE content varies based on histology and does so in a way that largely mimics the distribution of secondary elements seen in the EDS maps. The dentine of the samples is, with some exceptions, more strongly enriched than enamel. However, the enamel exhibits greater variability of enrichment within the same tissue; while it is generally the case that the outer enamel is more strongly enriched than the inner, both areas possess regions either more strongly or weakly enriched than would be predicted based on histology. Even within the same tooth this is the case, as seen in the Wonthaggi plesiosaur tooth. Here the inner enamel is split between areas of high REE concentration exceeding that of the enamel (approaching 10^3 ppm (log)), and exceptionally low concentration, between 10^{-1} ppm (log) for LREEs and 1ppm (log) for HREEs.

All the Australian Cretaceous samples exhibit a slightly “bell shaped” shale-normalized REE profile, with MREE being more abundant than LREE and HREE, though this is most

pronounced in the plesiosaur samples. The abundance of MREEs, and in particular Eu, is reflected in the Cathodoluminescence images. Strong MREE enrichment is associated with the overprinting of early diagenetic signals by later recrystallization and fractionation (Lécuyer *et al.* 2004). This pattern supports the interpretation of the specimens as well preserved, displaying minor REE adsorption from early diagenesis rather than the fractionated incorporation of REEs associated with later overprinting (Fadel *et al.* 2015; Žigaitė *et al.* 2015).

Cerium state varies greatly between tissue types. In Wonthaggi plesiosaur tooth the Ce anomaly of dentine appears to be influenced by a negative La anomaly, while the enamel is influenced by a positive La anomaly. The enamel of both plesiosaur teeth exhibits an overall positive Ce anomaly. The lungfish plate broadly displays no Ce anomaly. Positive La anomalies have been linked to riverine conditions (Kulaksız & Bau 2011). The HREE concentrations in our samples are lower than would be expected from ocean waters (Patrick *et al.* 2004). In the Svalbard fish material, REE enrichment is more varied. The Thelodont scales display a considerable positive Eu anomaly, which may be attributed to reworking during diagenesis (see Žigaitė *et al.* 2016).

Conclusions

The REE distribution patterns in the samples studied herein are indicative of minimal diagenetic overprint in the samples overall, with histological variations that overlap with the secondary element distributions seen from the EDS maps.

Our analysis supports the view that primary chemical composition of the fossil bioapatite is preserved in the studied specimens. In particular, the inner enamel of our samples likely consists of original tissues and is a prime candidate for future study. We are also able to show the

extent to which secondary elements had infiltrated these samples through diagenetic processes and identify their distribution. We conclude that histology is a better indicator of the extent of both preserved biominerals and secondary replacement than either diagenetic or non-histology-related biological factors.

The distribution of REEs in our samples in line with the interpretation of a freshwater system being present, in agreement with previous paleoenvironmental assessments. Our results provide no further insight into the climate of SE Australia in the Lower Cretaceous, though the cool environment identified by other studies (Rich *et al.* 2002) may have been a factor in the high level of preservation seen in our samples (Tütken *et al.* 2008). The elevated quantities of MREE in the Plesiosaur samples may be reflective of marine conditions inhabited by the animals in life (Žigaitė *et al.* 2016). Given the fluvial interpretation of the Eumeralla formation (Kear *et al.* 2006; Kear 2006; Benson *et al.* 2013), this further supports the idea of euryhaline behaviour in plesiosaurs (Benson *et al.* 2013; Bunker *et al.* 2022 and citations therein).

Mapping of REE and trace element distribution through electrospectroscopic techniques provides the benefit of visualising geochemical composition. In so doing, it allows for areas of significant alteration to be identified, providing insight into the mechanism of diagenetic change. Conversely, it highlights areas in which primary biomineral composition is likely to be preserved and thus serves as a useful tool to guide other analysis. In particular, mapping is likely to benefit the design and spatial targeting while conducting *in-situ* microanalyses. Consequently, the application of mapping from multiple sources increases confidence in biogeochemistry-based reconstructions of past organisms and environments.

Acknowledgements

The Authors would like express gratitude to the late Teressa Jeffries (NHMUK) for her invaluable assistance with conducting the LA-ICP-MS analyses, as well as Kerstin Lindén (NordSIM facility, Stockholm) for sample preparation. We are grateful to Thomas Rich and Tim Ziegler (Museums Victoria) and Patricia Vickers Rich (Monash University) for generous provision of the Australian samples, and likewise to Daniel Goujet and Gaël Clément (MNHN) for the Svalbard fossil material. We would like to thank Aleksander Kostka for his advice and assistance with EDX experimentation.

We are particularly grateful to Sophie Sanchez (Uppsala University), as well as Mary Kate Branigan (Uppsala University) and Ethan Killian for helpful discussions.

References

Amiot R, Buffetaut E, Lécuyer C, Wang X, Boudad L, Ding Z, Fourel F, Hutt S, Martineau F, Medeiros MA, Mo J, Simon L, Suteethorn V, Sweetman S, Tong H, Zhang F, Zhou Z. 2010. Oxygen isotope evidence for semi-aquatic habits among spinosaurid theropods. *Geology* 38:139–142. DOI: 10.1130/G30402.1.

Amiot R, Lécuyer C, Escarguel G, Billon-Bruyat J-P, Buffetaut E, Langlois C, Martin S, Martineau F, Mazin J-M. 2007. Oxygen isotope fractionation between crocodilian phosphate and water. *Palaeogeography, Palaeoclimatology, Palaeoecology* 243:412–420. DOI: 10.1016/j.palaeo.2006.08.013.

Barbin V. 2013. Application of cathodoluminescence microscopy to recent and past biological materials: a decade of progress. *Minerology and Petrology* 107:353–362.

Barrat J-A, Bayon G, Lalonde S. 2023. Calculation of cerium and lanthanum anomalies in geological and environmental samples. *Chemical Geology* 615:121202. DOI: 10.1016/j.chemgeo.2022.121202.

Bau M, Dulski P. 1996. Distribution of yttrium and rare-earth elements in the Penge and Kuruman iron-formations, Transvaal Supergroup, South Africa. *Precambrian Research* 79:37–55. DOI: 10.1016/0301-9268(95)00087-9

Benson RBJ, Fitzgerald EMG, Rich TH, Vickers-Rich P. 2013. Large freshwater plesiosaurian from the Cretaceous (Aptian) of Australia. *Alcheringa: An Australasian Journal of Palaeontology* 37:456–461. DOI: 10.1080/03115518.2013.772825.

Bernard A, Lécuyer C, Vincent P, Amiot R, Bardet N, Buffetaut E, Cuny G, Fourel F, Martineau F, Mazin J-M, Prieur A. 2010. Regulation of Body Temperature by Some Mesozoic Marine Reptiles. *Science* 328:1379–1382. DOI: 10.1126/science.1187443.

Blanc P, Baumer A, Cesbron F, Ohnenstetter D, Panczer G, Rémond G. 2000. Systematic Cathodoluminescence Spectral Analysis of Synthetic Doped Minerals: Anhydrite, Apatite, Calcite, Fluorite, Scheelite and Zircon. In: Pagel M, Barbin V, Blanc P, Ohnenstetter D eds. *Cathodoluminescence in Geosciences*. Berlin, Heidelberg: Springer, 127–160. DOI: 10.1007/978-3-662-04086-7_5.

Blom H, Goujet D. 2002. Thelodont Scales from the Lower Devonian Red Bay Group, Spitsbergen. *Palaeontology* 45:795–820. DOI: 10.1111/1475-4983.00261.

Blomeier D, Wisshak M, Dallmann W, Volohonsky E, Freiwald A. 2003. Facies analysis of the old Red Sandstone of Spitsbergen (Wood Bay Formation): Reconstruction of the depositional environments and implications of basin development. *Facies* 49:151–174. DOI: 10.1007/s10347-003-0030-1.

Bunker G, Martill DM, Smith RE, Zouhri S, Longrich N. 2022. Plesiosaurs from the fluvial Kem Kem Group (mid-Cretaceous) of eastern Morocco and a review of non-marine plesiosaurs. *Cretaceous Research* 140:105310. DOI: 10.1016/j.cretres.2022.105310.

Burton JH, Wright LE. 1995. Nonlinearity in the relationship between bone Sr/Ca and diet: Paleodietary implications. *American Journal of Physical Anthropology* 96:273–282. DOI: 10.1002/ajpa.1330960305.

Chen J, Algeo TJ, Zhao L, Chen Z-Q, Cao L, Zhang L, Li Y. 2015. Diagenetic uptake of rare earth elements by bioapatite, with an example from Lower Triassic conodonts of South China. *Earth-Science Reviews* 149:181–202. DOI: 10.1016/j.earscirev.2015.01.013.

~~Daniel~~ Bryant ~~J.~~, Froelich PN. 1995. A model of oxygen isotope fractionation in body water of large mammals. *Geochimica et Cosmochimica Acta* 59:4523–4537. DOI: 10.1016/0016-7037(95)00250-4.

De Rooij J, van der Lubbe JHJL, Verdegaal S, Hulscher M, Tooms D, Kaskes P, Verhage O, Portanger L, Schulp AS. 2022. Stable isotope record of Triceratops from a mass accumulation (Lance Formation, Wyoming, USA) provides insights into Triceratops behaviour and ecology. *Palaeogeography, Palaeoclimatology, Palaeoecology* 607:111274. DOI: 10.1016/j.palaeo.2022.111274.

525 Dumont M, Zoeger N, Streli C, Wobrauschek P, Falkenberg G, Sander PM, Pyzalla AR. 2009.
526 Synchrotron XRF analyses of element distribution in fossilized sauropod dinosaur bones.
527 *Powder Diffraction* 24:130–134. DOI: 10.1154/1.3131803.
528 Dumont M, Borbély A, Kostka A, Kaysser-Pyzalla A. 2011. Characterization of Sauropod Bone
529 Structure. In: Klein N, Remes K, Gee CT, Sander PM eds. *Biology of the Sauropod*
530 *dinosaurs: understanding the life of giants*. Bloomington: Indiana University Press, 150–
531 170.
532 Dumont M, Tütken T, Kostka A, Duarte MJ, Borodin S. 2014. Structural and functional
533 characterization of enamel pigmentation in shrews. *Journal of Structural Biology*
534 186:38–48. DOI: 10.1016/j.jsb.2014.02.006.
535 Eagle RA, Tütken T, Martin TS, Tripati AK, Fricke HC, Connely M, Cifelli RL, Eiler JM. 2011.
536 Dinosaur Body Temperatures Determined from Isotopic (13C-18O) Ordering in Fossil
537 Biominerals. *Science* 333:443–445. DOI: 10.1126/science.1206196.
538 Embleton BJJ, McElhinny MW. 1982. Marine magnetic anomalies, palaeomagnetism and the
539 drift history of Gondwanaland. *Earth and Planetary Science Letters* 58:141–150. DOI:
540 10.1016/0012-821X (82)90189-3.
541 Enax J, Prymak O, Raabe D, Epple M. 2012. Structure, composition, and mechanical properties
542 of shark teeth. *Journal of Structural Biology* 178:290–299. DOI:
543 10.1016/j.jsb.2012.03.012.
544 Fadel A, Žigaitė Ž, Blom H, Pérez-Huerta A, Jeffries T, Märss T, Ahlberg PE. 2015.
545 Palaeoenvironmental signatures revealed from rare earth element (REE) compositions of
546 vertebrate microremains of the Vesiku Bone Bed (Homerian, Wenlock), Saaremaa Island,
547 Estonia. *Estonian Journal of Earth Sciences* 64:36. DOI: 10.3176/earth.2015.07.
548 Fricke HC, Rogers RR, Backlund R, Dwyer CN, Echt S. 2008. Preservation of primary stable
549 isotope signals in dinosaur remains, and environmental gradients of the Late Cretaceous
550 of Montana and Alberta. *Palaeogeography, Palaeoclimatology, Palaeoecology* 266:13–
551 27. DOI: 10.1016/j.palaeo.2008.03.030.
552 Gaft M, Reisfeld R, Panczer G, Boulon G, Shoval S, Champagnon B. 1997. Accommodation of
553 rare-earths and manganese by apatite. *Optical Materials* 8:149–156. DOI:
554 10.1016/S0925-3467(97)00042-6.

555 Ghadimi E, Eimar H, Marelli B, Nazhat SN, Asgharian M, Vali H, Tamimi F. 2013. Trace
556 elements can influence the physical properties of tooth enamel. *SpringerPlus* 2:499. DOI:
557 10.1186/2193-1801-2-499.
558 Goedert J, Amiot R, Berthet D, Fourel F, Simon L, Lécuyer C. 2020. Combined oxygen and
559 sulphur isotope analysis—a new tool to unravel vertebrate (paleo)-ecology. *The Science*
560 *of Nature* 107:10. DOI: 10.1007/s00114-019-1664-3.
561 Goedert J, Lécuyer C, Amiot R, Arnaud-Godet F, Wang X, Cui L, Cuny G, Douay G, Fourel F,
562 Panczer G, Simon L, Steyer J-S, Zhu M. 2018. Euryhaline ecology of early tetrapods
563 revealed by stable isotopes. *Nature* 558:68–72. DOI: 10.1038/s41586-018-0159-2.
564 Grandjean P, Cappetta H, Michard A, ~~Albare`de~~ F. 1987. The assessment of REE patterns and
565 143Nd/144Nd ratios in fish remains. *Earth and Planetary Science Letters* 84:181–196.
566 DOI: 10.1016/0012-821X (87)90084-7.
567 Götze J. 2012. Application of Cathodoluminescence Microscopy and Spectroscopy in
568 Geosciences. *Microscopy and Microanalysis* 18:1270–1284. DOI:
569 10.1017/S1431927612001122.
570 Habermann D, Götte T, Meijer J, Stephan A, Richter DK, Niklas JR. 2000. High resolution rare-
571 earth elements analyses of natural apatite and its application in geo-sciences: Combined
572 micro-PIXE, quantitative CL spectroscopy and electron spin resonance analyses. *Nuclear*
573 *Instruments and Methods in Physics Research Section B: Beam Interactions with*
574 *Materials and Atoms* 161–163:846–851. DOI: 10.1016/S0168-583X(99)00998-2.
575 Heuser A, Tütken T, Gussone N, Galer SJG. 2011. Calcium isotopes in fossil bones and teeth –
576 Diagenetic versus biogenic origin. *Geochimica et Cosmochimica Acta* 75: 3419-3433.
577 DOI: 10.1016/j.gca.2010.03.032.
578 Herwartz D, Tütken T, Münker C, Jochum KP, Stoll B, Sander PM. 2011. Timescales and
579 mechanisms of REE and Hf uptake in fossil bones. *Geochimica et Cosmochimica Acta*
580 75: 82–105. DOI: 10.1016/j.gca.2010.09.036.
581 Herwartz D, Münker C, Tütken T, Hoffmann JE, Wittke A, Barbier B. 2013a. Lu–Hf isotope
582 systematics of fossil biogenic apatite and their effects on geochronology. *Geochimica et*
583 *Cosmochimica Acta* 101:328–343. DOI: 10.1016/j.gca.2012.09.049.

584 Herwartz D, Tütken T, Jochum KP, Sander PM. 2013b. Rare earth element systematics of fossil
585 bone revealed by LA-ICPMS analysis. *Geochimica et Cosmochimica Acta* 103:161–183.
586 DOI: 10.1016/j.gca.2012.10.038.
587 Hoppe KA, Koch PL, Furutani TT. 2003. Assessing the preservation of biogenic strontium in
588 fossil bones and tooth enamel. *International Journal of Osteoarchaeology* 13:20–28.
589 DOI: 10.1002/oa.663.
590 Hättig K, Stevens K, Thies D, Schweigert G, Mutterlose J. 2019. Evaluation of shark tooth
591 diagenesis-screening methods and the application of their stable oxygen isotope data for
592 palaeoenvironmental reconstructions. *Journal of the Geological Society* 176: 482-49.
593 DOI: 10.1144/jgs2018-19.
594 Ivanova V, Shchetnikov A, Semeney E, Filinov I, Simon K. 2022. LA-ICP-MS analysis of rare
595 earth elements in tooth enamel of fossil small mammals (Ust-Oda section, Fore-Baikal
596 area, Siberia): paleoenvironmental interpretation. *Journal of Quaternary Science*
597 37:1246–1260. DOI: 10.1002/jqs.3428.
598 Johannesson KH, Hawkins DL, Cortés A. 2006. Do Archean chemical sediments record ancient
599 seawater rare earth element patterns? *Geochimica et Cosmochimica Acta* 70:871–890.
600 DOI: 10.1016/j.gca.2005.10.013.
601 Kear BP. 2006. Plesiosaur remains from Cretaceous high-latitude non-marine deposits in
602 southeastern Australia. *Journal of Vertebrate Paleontology* 26:196–199. DOI:
603 10.1671/0272-4634(2006)26[196:PRFCHN]2.0.CO;2.
604 Kear BP, Schroeder NI, Vickers-Rich P, Rich TH. 2006. Plesiosaur remains from Cretaceous
605 high-latitude non-marine deposits in southeastern Australia. *Journnal of Vertebrate*
606 *Paleontology* 26: 196-199.
607 Kear BP, Hamilton-Bruce RJ. 2011. *Dinosaurs in Australia: Mesozoic Life from the Southern*
608 *Continent*. Csiro Publishing.
609 Kear B, Larsson D, Lindgren J, Kundrat M. 2017. Exceptionally prolonged tooth formation in
610 elasmosaurid plesiosaurians. *PLOSOne*, 12(2):e0172759.
611 DOI:10.1371/journal.pone.0172759
612 Kear BP, Fordyce RE, Hiller N, Siversson M. 2018. A palaeobiogeographical synthesis of
613 Australasian Mesozoic marine tetrapods. *Alcheringa: An Australasian Journal of*
614 *Palaeontology* 42:461–486. DOI: 10.1080/03115518.2017.1397428.

615 Keenan SW, Engel AS, Roy A, Lisa Bovenkamp-Langlois G. 2015. Evaluating the consequences
616 of diagenesis and fossilization on bioapatite lattice structure and composition. *Chemical*
617 *Geology* 413:18–27. DOI: 10.1016/j.chemgeo.2015.08.005.
618 Kemp A. 2001. Petrodentine in derived Dipnoan tooth plates. *Journal of Vertebrate*
619 *Paleontology* 21:422–437. DOI: 10.1671/0272-4634(2001)021[0422:PIDDTP]2.0.CO;2.
620 Kemp A. 2002. Unique dentition of lungfish. *Microscopy Research and Technique* 59:435–448.
621 DOI: 10.1002/jemt.10221.
622 Kemp A, Trueman CN. 2003. Rare earth elements in Solnhofen biogenic apatite: geochemical
623 clues to the palaeoenvironment. *Sedimentary Geology* 155:109–127. DOI:
624 10.1016/S0037-0738(02)00163-X.
625 Kemp A. 2005. New insights into ancient environments using dental characters in Australian
626 Cenozoic lungfish. *Alcheringa: An Australasian Journal of Palaeontology* 29:123–149.
627 DOI: 10.1080/03115510508619564.
628 Kemp A, Barry JC. 2006. Prismatic dentine in the Australian lungfish, Neoceratodus forsteri
629 (Osteichthyes: Dipnoi). *Tissue and Cell* 38:127–140. DOI: 10.1016/j.tice.2006.01.001.
630 Klock C, Leuzinger L, Santucci RM, Martinelli AG, Marconato A, Marinho TS, Luz Z,
631 Vennemann T. 2022. A bone to pick: stable isotope compositions as tracers of food
632 sources and paleoecology for notosuchians in the Brazilian Upper Cretaceous Bauru
633 Group. *Cretaceous Research* 131:105113. DOI: 10.1016/j.cretres.2021.105113.
634 Kocsis L, Trueman CN, Palmer MR. 2010. Protracted diagenetic alteration of REE contents in
635 fossil bioapatites: Direct evidence from Lu–Hf isotope systematics. *Geochimica et*
636 *Cosmochimica Acta* 74:6077–6092. DOI: 10.1016/j.gca.2010.08.007.
637 Kohn MJ, Cerling TE. 2002. Stable Isotope Compositions of Biological Apatite. *Reviews in*
638 *Mineralogy and Geochemistry* 48:455–488. DOI: 10.2138/rmg.2002.48.12.
639 Kohn MJ, Schoeninger MJ, Barker WW. 1999. Altered states: effects of diagenesis on fossil
640 tooth chemistry. *Geochimica et Cosmochimica Acta* 63:2737–2747. DOI:
641 10.1016/S0016-7037(99)00208-2.
642 Kolodny Y, Luz B, Sander M, Clemens WA. 1996. Dinosaur bones: fossils or pseudomorphs?
643 The pitfalls of physiology reconstruction from apatitic fossils. *Palaeogeography,*
644 *Palaeoclimatology, Palaeoecology* 126:161–171. DOI: 10.1016/S0031-0182(96)00112-5.

Kulaksız S, Bau M. 2011. Rare earth elements in the Rhine River, Germany: First case of anthropogenic lanthanum as a dissolved microcontaminant in the hydrosphere. *Environment International* 37:973–979. DOI: 10.1016/j.envint.2011.02.018.

Lécuyer C, Reynard B, Grandjean P. 2004. Rare earth element evolution of Phanerozoic seawater recorded in biogenic apatites. *Chemical Geology* 204:63–102. DOI: 10.1016/j.chemgeo.2003.11.003.

Leuzinger L, Kocsis L, Luz Z, Vennemann T, Ulyanov A, Fernández M. 2022. Latest Maastrichtian middle- and high-latitude mosasaurs and fish isotopic composition: carbon source, thermoregulation strategy, and thermal latitudinal gradient. *Paleobiology*:1–21. DOI: 10.1017/pab.2022.38.

Li F, Li H, Yang Z, D. Huang T, Wu D, Wang S. 2021. Rapid online fractionated analyses of rare earth elements in a dinosaur fossil by mass spectrometry. *Journal of Analytical Atomic Spectrometry* 36:2612–2616. DOI: 10.1039/D1JA00265A.

Lübke A, Enax J, Loza K, Prymak O, Gaengler P, Fabritius H-O, Raabe D, Epple M. 2015. Dental lessons from past to present: ultrastructure and composition of teeth from plesiosaurs, dinosaurs, extinct and recent sharks. *RSC Advances* 5:61612–61622. DOI: 10.1039/C5RA11560D.

Lübke A, Loza K, Patnaik R, Enax J, Raabe D, Prymak O, Fabritius H-O, Gaengler P, Epple M. 2017. Reply to the ‘Comments on “Dental lessons from past to present: ultrastructure and composition of teeth from plesiosaurs, dinosaurs, extinct and recent sharks”’ by H. Botella et al. , RSC Adv. , 2016, 6 , 74384–74388. *RSC Advances* 7:6215–6222. DOI: 10.1039/C6RA27121A.

Martin AJ, Rich TH, Hall M, Vickers-Rich P, Vazquez-Prokopec G. 2012. A polar dinosaur-track assemblage from the Eumeralla Formation (Albian), Victoria, Australia. *Alcheringa: An Australasian Journal of Palaeontology* 36:171–188. DOI: 10.1080/03115518.2011.597564.

McLennan SM. 1989. Rare earth elements in sedimentary rocks; influence of provenance 28 and sedimentary processes. *Reviews in Mineralogy and Geochemistry* 21:169–200.

Mutter JC, A. Hegarty K, Cande SC, Weissel JK. 1985. Breakup between Australia and Antarctica: A brief review in the light of new data. *Tectonophysics* 114:255–279. DOI: 10.1016/0040-1951(85)90016-2.

Ørvig T. 1967. Some new acanthodian material from the Lower Devonian of Europe. *Zoological Journal of the Linnean Society* 47:131–153. DOI: 10.1111/j.1096-3642.1967.tb01400.x.

Owocki K, Kremer B, Cotte M, Bocherens H. 2020. Diet preferences and climate inferred from oxygen and carbon isotopes of tooth enamel of Tarbosaurus bataar (Nemegt Formation, Upper Cretaceous, Mongolia). *Palaeogeography, Palaeoclimatology, Palaeoecology* 537:109190. DOI: 10.1016/j.palaeo.2019.05.012.

Patrick D, Martin JE, Parris DC, Grandstaff DE. 2004. Paleoenvironmental interpretations of rare earth element signatures in mosasaurs (reptilia) from the upper Cretaceous Pierre Shale, central South Dakota, USA. *Palaeogeography, Palaeoclimatology, Palaeoecology* 212:277–294. DOI: 10.1016/j.palaeo.2004.06.005.

Poropat SF, Bell PR, Hart LJ, Salisbury SW, Kear BP. 2023. An annotated checklist of Australian Mesozoic tetrapods. *Alcheringa: An Australasian Journal of Palaeontology* 47:129–205. DOI: 10.1080/03115518.2023.2228367.

Poropat SF, Martin SK, Tosolini A-MP, Wagstaff BE, Bean LB, Kear BP, Vickers-Rich P, Rich TH. 2018. Early Cretaceous polar biotas of Victoria, southeastern Australia—an overview of research to date. *Alcheringa: An Australasian Journal of Palaeontology* 42:157–229. DOI: 10.1080/03115518.2018.1453085.

Rey K, Amiot R, Fourel F, Abdala F, Fluteau F, Jalil N-E, Liu J, Rubidge BS, Smith RM, Steyer JS, Viglietti PA, Wang X, Lécuyer C. 2017. Oxygen isotopes suggest elevated thermometabolism within multiple Permo-Triassic therapsid clades. *eLife* 6:e28589. DOI: 10.7554/eLife.28589.

Reynard B, Lécuyer C, Grandjean P. 1999. Crystal-chemical controls on rare-earth element concentrations in fossil biogenic apatites and implications for paleoenvironmental reconstructions. *Chemical Geology* 155:233–241. DOI: 10.1016/S0009-2541(98)00169-7.

Rich TH, Vickers-Rich P, Gangloff RA. 2002. Polar Dinosaurs. *Science* 295:979–980. DOI: 10.1126/science.1068920.

Richard M, Pons-Branchu E, Carmieli R, Kaplan-Ashiri I, Alvaro Gallo A, Ricci G, Caneve L, Wroth K, Dapoigny A, Tribolo C, Boaretto E, Toffolo MB. 2022. Investigating the effect of diagenesis on ESR dating of Middle Stone Age tooth samples from the open-air site of Lovedale, Free State, South Africa. *Quaternary Geochronology* 69:101269. DOI: 10.1016/j.quageo.2022.101269.

Romilio A, Godfrey T. 2022. A new dinosaur tracksite from the Lower Cretaceous (Aptian–Albian) Eumeralla Formation of Wattle Hill, Victoria, Australia: a preliminary investigation. *Historical Biology* 34:2315–2323. DOI: 10.1080/08912963.2021.2014481.

Sasagawa I, Ishiyama M, Yokosuka H, Mikami M, Uchida T. 2009. Tooth enamel and enameloid in actinopterygian fish. *Frontiers of Materials Science in China* 3:174–182. DOI: 10.1007/s11706-009-0030-3

Schoeninger MJ, Hallin K, Reeser H, Valley JW, Fournelle J. 2003. Isotopic alteration of mammalian tooth enamel. *International Journal of Osteoarchaeology* 13:11–19. DOI: 10.1002/oa.653.

Ségalen L, de Rafélis M, Lee-Thorp JA, Maurer A-F, Renard M. 2008. Cathodoluminescence tools provide clues to depositional history in Miocene and Pliocene mammalian teeth. *Palaeogeography, Palaeoclimatology, Palaeoecology* 266:246–253.

Séon N, Amiot R, Martin JE, Young MT, Middleton H, Fourel F, Picot L, Valentin X, Lécuyer C. 2020. Thermophysiologies of Jurassic marine crocodylomorphs inferred from the oxygen isotope composition of their tooth apatite. *Philosophical Transactions of the Royal Society B: Biological Sciences* 375:20190139. DOI: 10.1098/rstb.2019.0139.

Shaw HF, Wasserburg GJ. 1985. Sm-Nd in marine carbonates and phosphates: Implications for Nd isotopes in seawater and crustal ages. *Geochimica et Cosmochimica Acta* 49:503–518. DOI: 10.1016/0016-7037(85)90042-0.

Smith MM & Krupina NI. 2001. Conserved developmental processes constrain evolution of lungfish dentitions. *Journal of Anatomy*, 199:161-168.

Thibon F, Goedert J, Séon N, Weppe L, Martin JE, Amiot R, Adnet S, Lambert O, Bustamante P, Lécuyer C, Vigier N. 2022. The ecology of modern and fossil vertebrates revisited by lithium isotopes. *Earth and Planetary Science Letters* 599:117840. DOI: 10.1016/j.epsl.2022.117840.

734 Toyoda K, Tokonami M. 1990. Diffusion of rare-earth elements in fish teeth from deep-sea
735 sediments. *Nature* 345:607–609. DOI: 10.1038/345607a0.
736 Tossolini A-MP, Korasidis, VA, Wagstaff BE, Cantrill DJ, Gallagher, SJ, Norvick MS. 2018.
737 Palaleoenvironments and palaeocommunities from Lower Cretaceous high-latitude sites,
738 Otway, southeastern Australia. *Palaeogeography Palaeoclimatology Palaeoecology*
739 496:62–84. DOI: 10.1016/j.palaeo.2018.01.017.
740 Trotter JA, Eggins SM. 2006. Chemical systematics of conodont apatite determined by laser
741 ablation ICPMS. *Chemical Geology* 233:196–216. DOI: 10.1016/j.chemgeo.2006.03.004.
742 Trueman CN. 1999. Rare earth element geochemistry and taphonomy of terrestrial vertebrate
743 assemblages. *Palaios* 14:555–568.
744 Trueman CN. 2013. Chemical taphonomy of biomineralized tissues. *Palaeontology* 56:475–486.
745 DOI: 10.1111/pala.12041.
746 Trueman CN, Behrensmeyer AK, Potts R, Tuross N. 2006. High-resolution records of location
747 and stratigraphic provenance from the rare earth element composition of fossil bones.
748 *Geochimica et Cosmochimica Acta* 70:4343–4355. DOI: 10.1016/j.gca.2006.06.1556.
749 Trueman CN, Palmer MR. 1997. Diagenetic Origin of REE in Vertebrate Apatite: A
750 Reconsideration of Samoilov and Benjamini, 1996. *PALAIOS* 12:495–497. DOI:
751 10.2307/3515387.
752 Trueman CN, Tuross N. 2002. Trace Elements in Recent and Fossil Bone Apatite. *Reviews in*
753 *Mineralogy and Geochemistry* 48:489–521. DOI: 10.2138/rmg.2002.48.13.
754 Tütken T, Vennemann TW, Pfretzschner H-U. 2008. Early diagenesis of bone and tooth apatite
755 in fluvial and marine settings: Constraints from combined oxygen isotope, nitrogen and
756 REE analysis. *Palaeogeography Palaeoclimatology Palaeoecology* 266:254–268. DOI:
757 10.1016/j.palaeo.2008.03.037.
758 Volohonsky E, Wisshak M, Blomeier D, Seilacher A, Snigirevsky S. 2008. A new helical trace
759 fossil from the Lower Devonian of Spitsbergen (Svalbard) and its palaeoenvironmental
760 significance. *Palaeogeography, Palaeoclimatology, Palaeoecology* 267:17–20. DOI:
761 10.1016/j.palaeo.2008.04.011.
762 Wagstaff BE, Mason JM. 1989. Palynological dating of Lower Cretaceous coastal vertebrate
763 localities, Victoria, Australia. National Geographic Society Research Reports 5:54–63.

764 Wagstaff BE, Gallagher SJ, Hall WM, Korasidis VA, Rich TH, Seegets-Villiers DE, Vickers-
765 Rich PA. 2020. Palynological-age determination of Early Cretaceous vertebrate-bearing
766 beds along the south Victorian coast of Australia, with implications for the spore-pollen
767 biostratigraphy of the region. *Alcheringa: An Australasian Journal of Palaeontology*
768 44:460–474. DOI: 10.1080/03115518.2020.1754464.
769 Williams CT, Henderson P, Marlow CA, Molleson TI. 1997. The environment of deposition
770 indicated by the distribution of rare earth elements in fossil bones from Olduvai Gorge,
771 Tanzania. *Applied Geochemistry* 12:537–547. DOI: 10.1016/S0883-2927(97)00033-4.
772 Wright J, Schrader H, Holser WT. 1987. Paleoredox variations in ancient oceans recorded by
773 rare earth elements in fossil apatite. *Geochimica et Cosmochimica Acta* 51:631–644.
774 DOI: 10.1016/0016-7037(87)90075-5.
775 Žigaitė Ž, Karatajūtė-Talimaa V, Goujet D, Blom H. 2013. Thelodont scales from the Lower and
776 Middle Devonian Andrée Land Group, Spitsbergen. *GFF* 135:57–73. DOI:
777 10.1080/11035897.2012.762549.
778 Žigaitė, Ž., Fadel, A., Blom, H., Perez-Huerta, A., Jeffries, T., Märss, T., and Ahlberg, P.E.
779 2015. Rare earth elements (REEs) in vertebrate microremains from the upper Pridoli
780 Ohesaare beds of Saaremaa Island, Estonia: geochemical clues to palaeoenvironmnet.
781 Estonian Journal of Earth Sciences, 64: 115–120.
782 Žigaitė Ž, Fadel A, Pérez-Huerta A, Jeffries T, Goujet D, Ahlberg P. 2016. Palaeoenvironments
783 revealed by rare-earth element systematics in vertebrate bioapatite from the Lower
784 Devonian of Svalbard. *Canadian journal of earth sciences (Print)* 53:788–794.
785 Žigaitė Ž, Clément, G, Goujet D, Blom H. (*in prep*). New vertebrates from the Lower and
786 Middle Devonian of Andrée Land Group, Spitsbergen. *Geodiversitas*.
787
788
789
790
791
792
793
794

795
796
797
798
799

Figure 1

Cross-section drawings of general structures of the materials studied

(A) Plesiosaur tooth schema and transverse section showing enamel, dentine and dentine tubule. (B) Lungfish plate with longitudinal section showing the dentine composing the structure and the denteon . (C) Chondrichthyan scale with longitudinal section showing the enameloid , dentine and dentine tubule . (D) Thelodont scale with lateral section. EDJ – enamel-dentine junction.

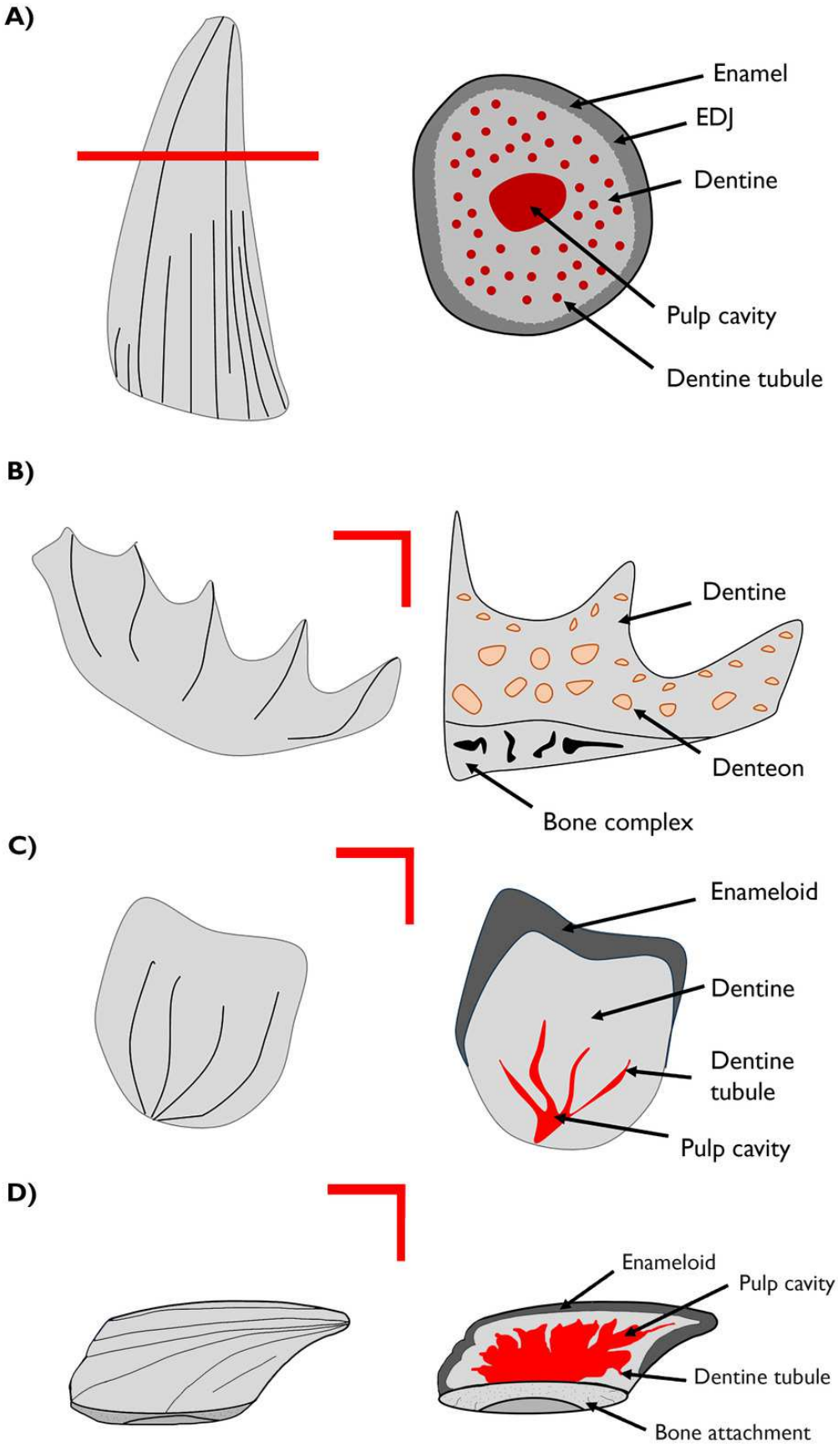
A)
Enamel
EDJ
Dentine
Pulp cavity
Dentine tubule
B)
Dentine
Denteon
Bone complex
C)
Enameloid
Dentine
Dentine tubule
Pulp cavity
D)
Enameloid
Pulp cavity
Dentine tubule
Bone attachment

Figure 2

Visible light photographs (VL) and optical cathodoluminescence (CL) images of fossil vertebrate hard tissues.

Plesiosaur teeth (A,B) and lungfish dental plates (C,D) from the Cretaceous ~~age~~ Eumeralla formation, Otway basin, Australia. Fish scales from the Devonian of Svalbard, Norway, including a chondrichthyan (E) and two thelodont body scales from Gråkammen (F) and Tavlefjellet (G). Teal dots on Svalbard specimens indicate LA-ICP-MS points.

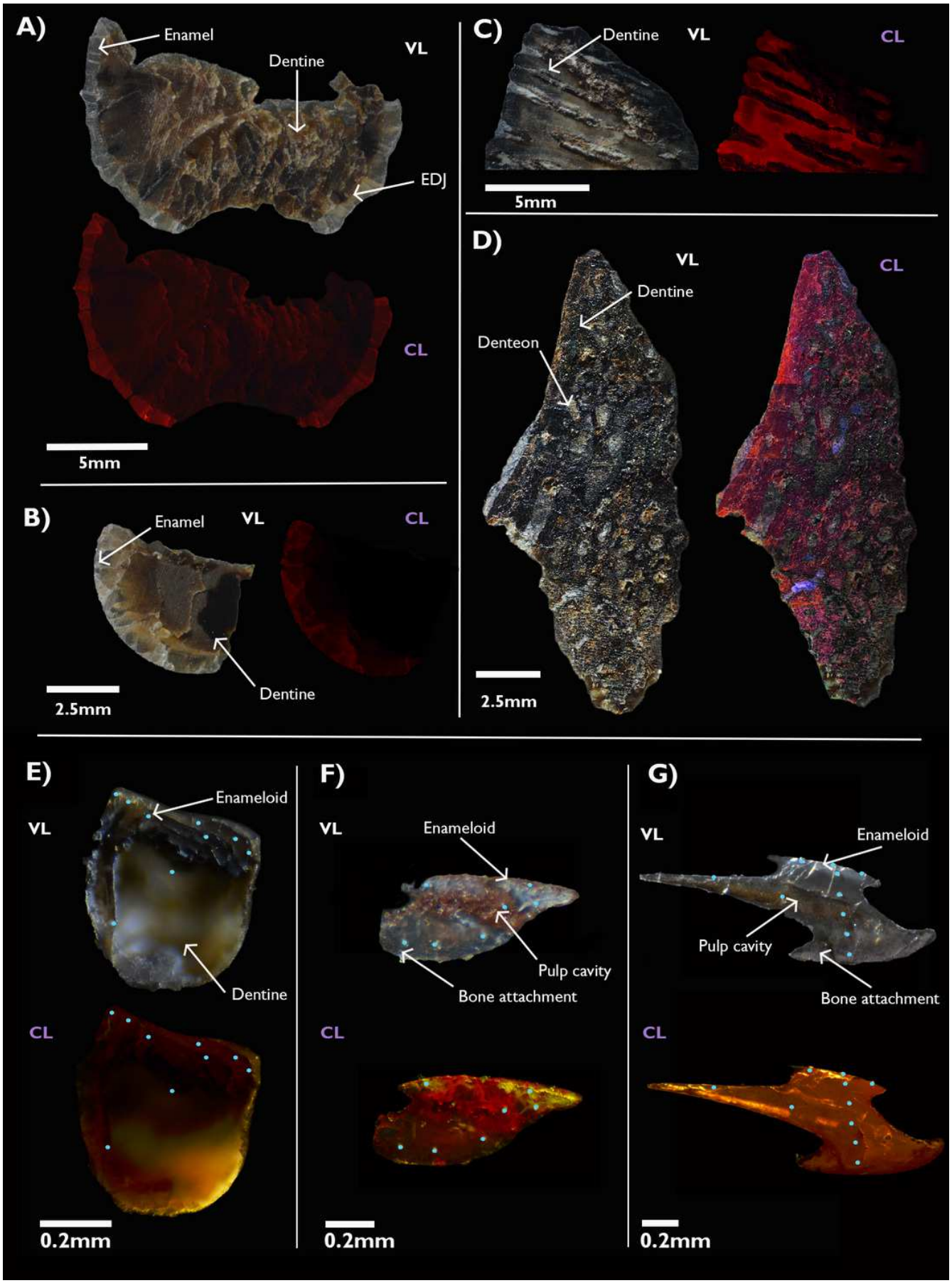
A)
Enamel
Dentine
VL
EDJ
CL
5mm
B)
Enamel
VL
CL
Dentine
2.5mm
C)
Dentine
VL
CL
5mm
D)
VL
CL
Dentine
Denteon
2.5mm
E)
Enameloid
VL
Dentine
CL
0.2mm
F)
VL
Enameloid
Pulp cavity
Bone attachment
CL
0.2mm
G)
VL
Enameloid
Pulp cavity
Bone attachment
CL
0.2mm

Figure 3

Shale-Normalized REE profiles of vertebrate hard tissues.

The profiles show in-situ data points for each tissue type and the Enamel-Dentine Junction, obtained through LA-ICP-MS. Due to the absence of enamel in the lungfish dental plate, data points have been divided between sites close to cracks and those further away, to determine whether this proximity affects REE uptake.

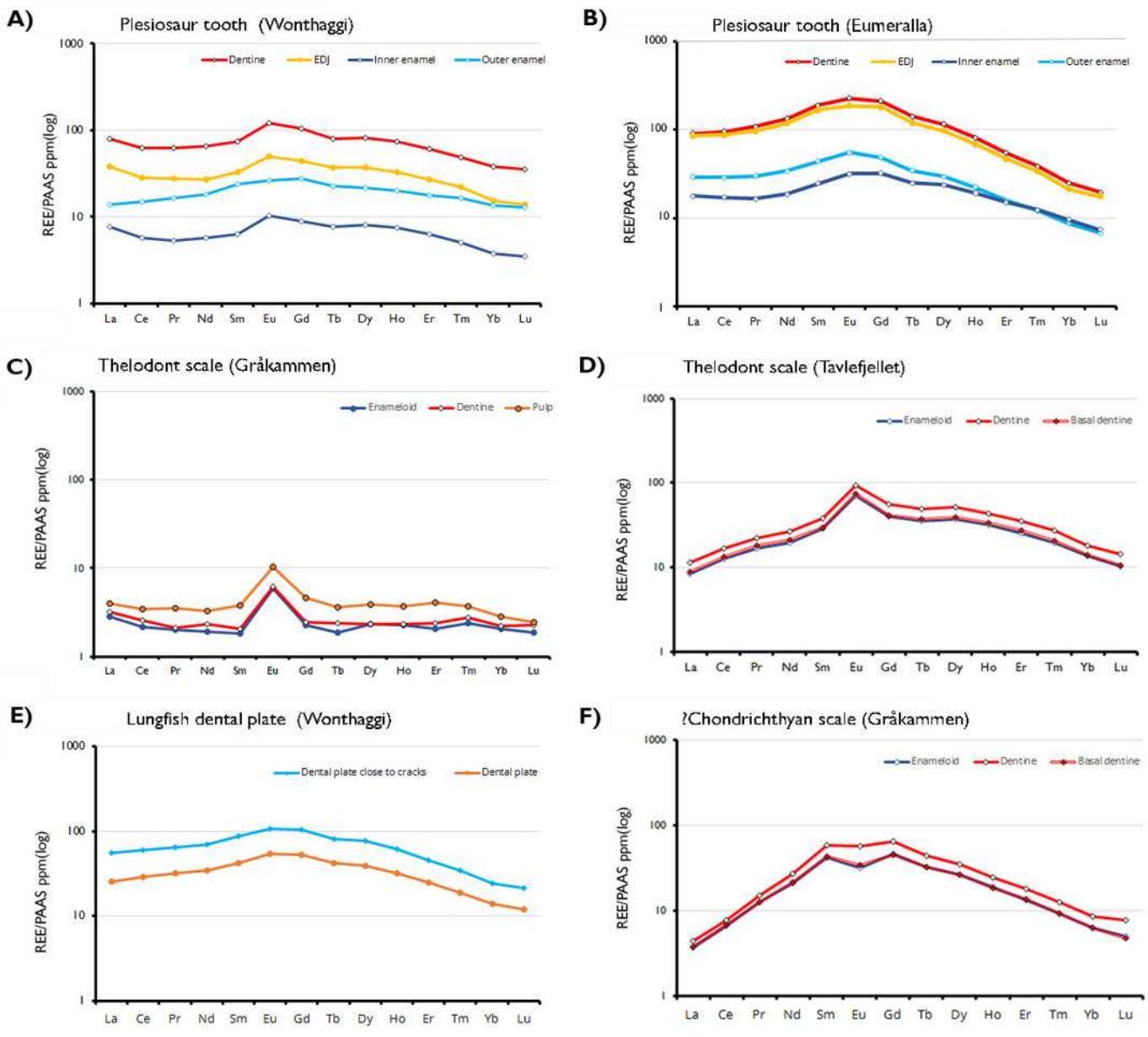

Figure 4

Plots of Ce/Ce*SN / vs Pr/Pr*SN plots with fields indicating potential Ce and La anomalies.

Ce/Ce*SN / vs Pr/Pr*SN for the Wonthaggi plesiosaur (A), Eumeralla plesiosaur (B) and lungfish dental plate (C**)**. $Ce/Ce^* = 2CeSN/(La_{SN} + Nd_{SN})$ and $Pr/Pr^* = 2Pr_{SN}/(Ce_{SN} + Sm_{SN})$; Field I: no anomaly; IIa: positive La-anomaly causes apparent negative Ce-anomaly; IIb: negative La-anomaly causes apparent positive Ce anomaly; IIIa: real positive Ce anomaly; IIIb: real negative Ce anomaly; IV: positive La-anomaly disguises positive Ce anomaly. After Bau & Dulski (1996).

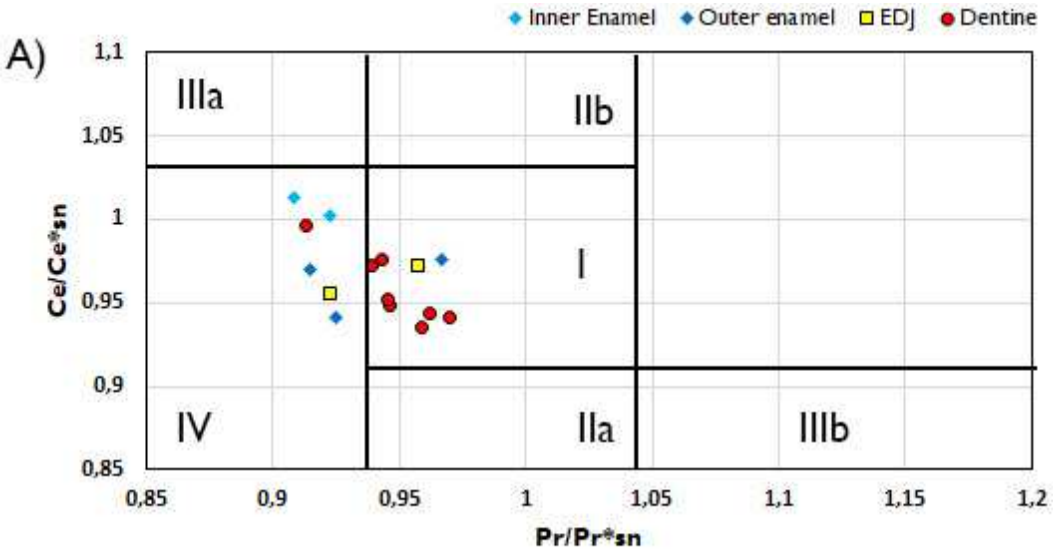
Inner Enamel
Outer enamel
EDJ
Dentine
A)
IIIa
IIb
I
IV
IIa
IIIb
Ce/Ce*sn
Pr/Pr*sn
1,1
1,05
1
0,95
0,9
0,85
0,85
0,9
0,95
1
1,05
1,1
1,15
1,2

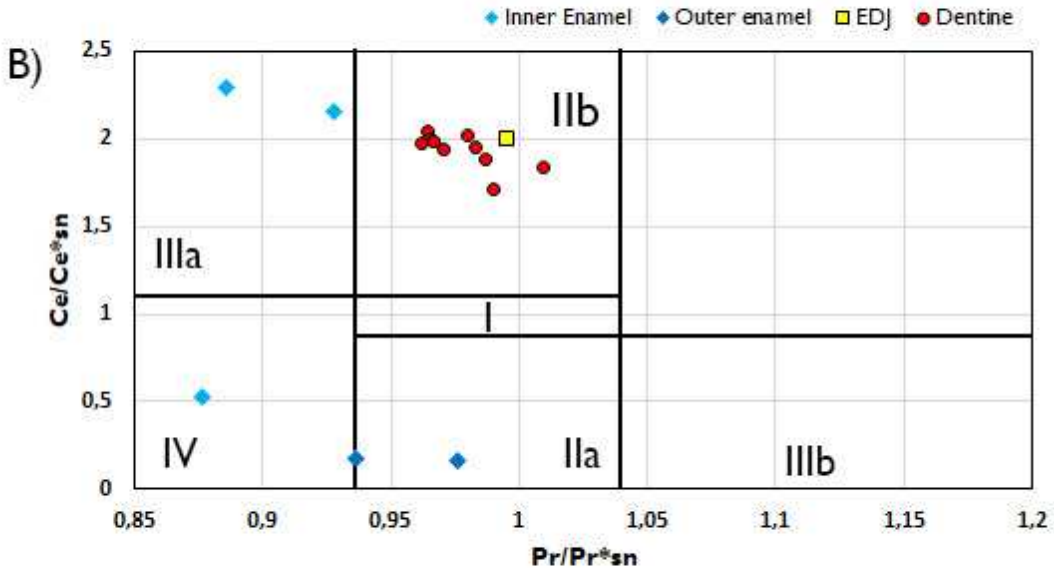
Inner Enamel
Outer enamel
EDJ
Dentine
B)
IIb
IIIa
I
IV
IIa
IIIb
Ce/Ce*sn
Pr/Pr*sn
2,5
2
1,5
1
0,5
0
0,85
0,9
0,95
1
1,05
1,1
1,15
1,2

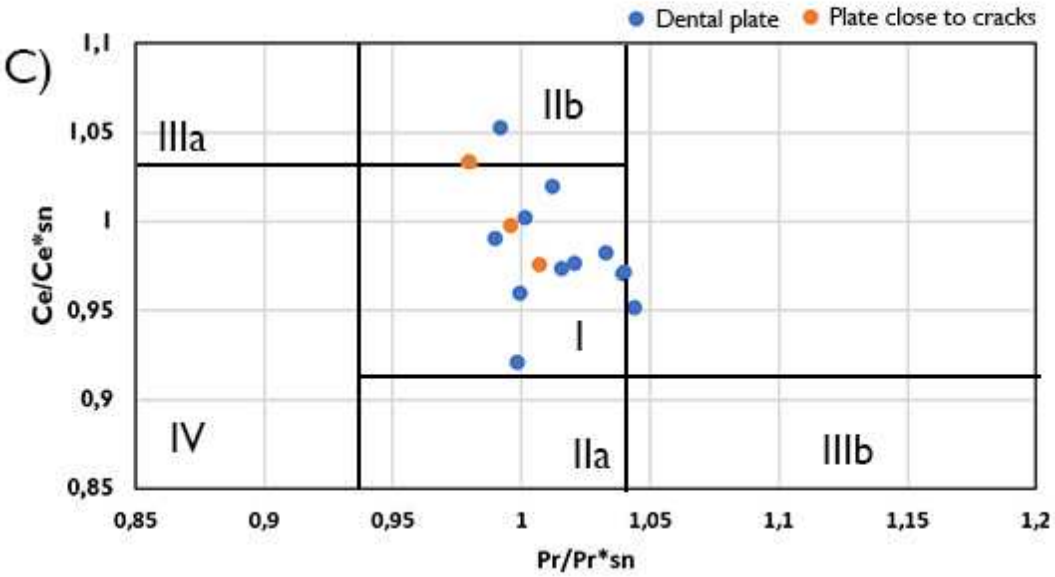
Dental plate
Plate close to cracks
C)
IIb
IIIa
I
IV
IIa
IIIb
Ce/Ce*sn
Pr/Pr*sn
1,1
1,05
1
0,95
0,9
0,85
0,85
0,9
0,95
1
1,05
1,1
1,15
1,2